

Numerical simulation of the transport and flow problems in perforated domains using generalized multiscale finite element method

Cite as: AIP Conference Proceedings **2025**, 100001 (2018); <https://doi.org/10.1063/1.5064930>
Published Online: 25 October 2018

V. Alekseev, U. Gavrilava, D. Spiridonov, A. Tyrylgin, and M. Vasilyeva



View Online



Export Citation

ARTICLES YOU MAY BE INTERESTED IN

[Mathematical modeling of the fluid flow and geo-mechanics in the fractured porous media using generalized multiscale finite element method](#)

AIP Conference Proceedings **2025**, 100009 (2018); <https://doi.org/10.1063/1.5064938>

[Multiscale model reduction of the flow problem in fractured porous media using mixed generalized multiscale finite element method](#)

AIP Conference Proceedings **2025**, 100008 (2018); <https://doi.org/10.1063/1.5064937>

[Numerical homogenization for wave propagation in fractured media](#)

AIP Conference Proceedings **2025**, 100002 (2018); <https://doi.org/10.1063/1.5064931>



Your Qubits. Measured.

Meet the next generation of quantum analyzers

- Readout for up to 64 qubits
- Operation at up to 8.5 GHz, mixer-calibration-free
- Signal optimization with minimal latency

[Find out more](#)



Numerical Simulation of the Transport and Flow Problems in Perforated Domains Using Generalized Multiscale Finite Element Method

V. Alekseev^{1,a)}, U. Gavrilova¹, D. Spiridonov¹, A. Tyrylgina¹ and M. Vasilyeva^{1,2}

¹*MMR Laboratory, North-Eastern Federal University, Yakutsk, Russia*

²*ISC, Texas A&M University, College Station, TX, USA*

^{a)}Corresponding author: alekseev.valen@mail.ru

Abstract. In this work, we consider flow and transport processes in perforated domains. Such processes have multiscale nature and occur in many real world applications, for example, in simulation of the carbonate reservoirs. The transport process is described by the convection-diffusion equation. The convection term in the transport equation is governed by a flow velocity field. The flow is described by Darcy equation. Numerical solutions for flow and transport equations in perforated domains are expensive and require resolving fine-scale details (perforations). For this reason, some type of model reduction is necessary. For coarse grid approximation, we use Generalized Multiscale Finite Element method (GMsFEM) for flow problem and construct local multiscale basis functions. We present numerical results for model problem in two-dimensional perforated domains.

INTRODUCTION

Many processes in porous media have multiscale nature. Numerical solutions are require resolving fine-scale details and some type of model reduction is needed. Model reduction techniques usually depend on a coarse grid approximation, which can be obtained by discretizing the problem on a coarse grid and choosing a suitable coarse-grid formulation of the problem [1, 2, 3, 4, 5, 6].

In this paper, we consider a Generalized Multiscale Finite Element Method (GMsFEM) for a flow problem in perforated domain, where the flow equation is described by Darcy equation. After solution of the flow problem using multiscale solver, we solve transport problem on a fine grid using Galerkin finite element method with numerical stabilization. In our approach, we use a mixed formulation for the flow problem. The use of a mixed formulation guarantees the mass conservation. In the mixed formulation, we first define snapshot spaces that represents the solution space in each coarse region. Next, we perform a local spectral decomposition in snapshot space to identify multiscale basis functions. For the pressure, we use piecewise constant basis functions. We consider two examples with homogeneous and heterogeneous permeabilities and perform numerical investigation of the errors for different number of multiscale basis functions.

The paper organized as follows. In Section 2, we present problem formulation. We describe fine and coarse grids approximation in Sections 3 and 4. In Section 5, we present numerical results and give conclusion.

PROBLEM FORMULATION

We consider flow and transport problem in perforated domain $\Omega_\epsilon = \Omega \setminus \mathcal{B}_\epsilon$, where \mathcal{B}_ϵ is the perforations [7]. The flow equation for the velocity field is described by the Darcy problem in domain Ω_ϵ

$$\begin{aligned} k^{-1}u + \nabla p &= 0, & x \in \Omega_\epsilon \\ \nabla \cdot u &= 0, & x \in \Omega_\epsilon, \end{aligned} \tag{1}$$

where $k = \frac{\kappa}{\mu}$, μ is viscosity, κ is permeability of a porous medium. We consider a flow problem with zero Dirichlet boundary condition on global boundary and set zero velocity on perforations.

Transport equation is described by a convection-diffusion equation for the concentration

$$\frac{\partial c}{\partial t} + u \nabla c - \nabla \cdot (D \nabla c) = f, \quad x \in \Omega_\epsilon, \quad (2)$$

where D is the diffusion coefficient, f is the source term and u is the velocity field. We consider transport equation with the homogeneous Neumann boundary conditions and the initial condition $c(x, 0) = c_0$ in Ω_ϵ for $t = 0$.

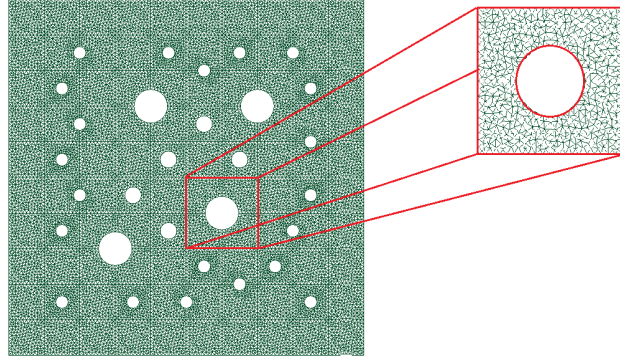


FIGURE 1. Illustration of the perforated domain Ω_ϵ with unstructured fine grid

FINE GRID APPROXIMATION

For numerical solution on the fine grid, we use finite element method [8]. Let

$$V = \{v \in L^2(\Omega_\epsilon)^d : \operatorname{div} v \in L^2(\Omega_\epsilon)\}, \quad Q = L^2(\Omega_\epsilon).$$

We consider two-dimensional problems with $d = 2$.

The weak formulation of the flow problem: find $(u, p) \in V \times Q$ such that

$$\begin{aligned} a(u, v) + b(p, v) &= 0 \quad \forall v \in V \\ b(u, q) &= 0 \quad \forall q \in Q, \end{aligned} \quad (3)$$

where

$$a(u, v) = - \int_{\Omega_\epsilon} k^{-1} u \cdot v \, dx, \quad b(u, p) = \int_{\Omega_\epsilon} p \nabla \cdot u \, dx,$$

For the approximation on the fine grid, we assume that the computational domain is discretized into triangles so that all perforations can be resolved by grid.

We can write approximation of the Darcy problem in the matrix form

$$\begin{pmatrix} A & B^T \\ B & 0 \end{pmatrix} \begin{pmatrix} u \\ p \end{pmatrix} = \begin{pmatrix} 0 \\ 0 \end{pmatrix}. \quad (4)$$

where we used the Raviart-Thomas space for velocity and the piecewise constant element for pressure in the fine-scale system.

To define the weak formulation for transport equation, we use finite element method. We have following weak formulation of the transport equation: find $c \in W$ such that

$$\frac{1}{\tau} m(c - \check{c}, r) + s(c, r) + d(c, r) = (f, r) \quad \forall r \in W \quad (5)$$

where $W = L^2(\Omega_\epsilon)$ and

$$m(c, r) = \int_{\Omega_\epsilon} c r dx, \quad s(c, r) = \int_{\Omega_\epsilon} u \cdot c r dx, \quad d(c, r) = \int_{\Omega_\epsilon} \nabla c \cdot \nabla r dx.$$

Here, for the time discretization we used an implicit scheme and \check{c} is the concentration in the previous time step and τ is the time step.

We can write (5) as the following matrix form

$$M \frac{c - \check{c}}{\tau} + (S + D)c = F, \quad (6)$$

where we use linear basis functions for approximation on the fine grid.

For the case, when convective term dominates over diffusion, the standard approximation using classical Galerkin method can lead to oscillations in the solution of the problem. For the numerical simulation, we use a stabilization method (Streamline-Upwinded Petrov-Galerkin method, SUPG). In the SUPG method, we have following variational formulation of the transport equation: find $c \in W$ such that

$$\frac{1}{\tau} m(c - \check{c}, \check{r}) + s(c, \check{r}) + d(c, \check{r}) = (f, \check{r}) \quad \forall \check{r} \in W \quad (7)$$

where $\check{r} = (r + \frac{h}{2|u|} u \Delta r)$ and h is the mesh size.

COARSE GRID APPROXIMATION USING GMsFEM

Next, we describe construction of the coarse grid approximation using Generalized finite element method (GMsFEM) for flow problem.[9] Note that, we solve a transport problem on the fine grid and construct multiscale solver for flow problem only.

Let \mathcal{T}_H be a coarse grid of the computational domain Ω_ϵ with coarse grid size H . Let \mathcal{E}_H be the set of all edges of the coarse grid and N_E be the total number of edges and $\mathcal{E}_H = \bigcup_{i=1}^{N_E} E_i$. As local domain, we define the neighborhood of the edge $E \in \mathcal{E}_H$ (see Figure 2)

$$\omega^\epsilon = \bigcup_j \{K_j \in \mathcal{T}^H \mid E \in \partial K_j\},$$

where K_j is the coarse grid cell [1, 2].

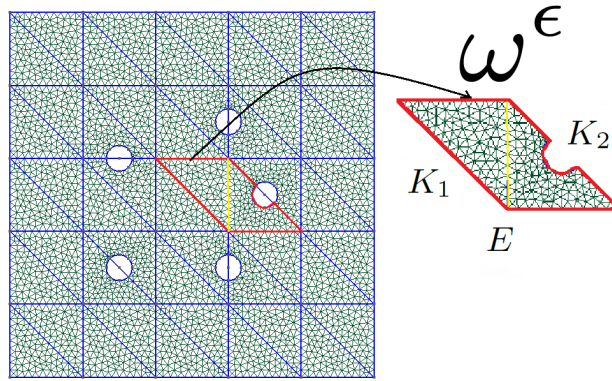


FIGURE 2. Illustrations of the coarse grid \mathcal{T}_H and local domain $\omega^\epsilon = K_1 \cup K_2$ for the coarse edge E

We construct an multiscale space for the velocity $u_c \in V_{ms}$

$$V_{ms} := \text{span}\{\psi_1, \dots, \psi_{N_c}\},$$

where ψ_i is the multiscale basis functions that supported in a local domain ω^ϵ ($i = 1, \dots, N_c$), and N_c is the number of basis functions. For the pressure, we use the space of piecewise constant functions Q_{ms} over the coarse triangulation \mathcal{T}_H .

We start with construction of the a snapshot space in ω^ϵ and after that perform a dimension reduction by solution of the local spectral problem. The purpose of this is to determine the dominant modes in the snapshot space and to obtain a small dimension space for the approximation the solution.

For the snapshot space construction, we solve local problem on the domain ω^ϵ : find $(\phi_j, \eta) \in V_h^{\omega^\epsilon} \times Q_h^{\omega^\epsilon}$ such that

$$\begin{aligned} \int_{\omega^\epsilon} k^{-1} \phi_j v dx - \int_{\omega^\epsilon} \eta \nabla \cdot v dx &= 0, \quad v \in V_h^{\omega^\epsilon}, \\ \int_{\omega^\epsilon} r \nabla \cdot \phi_j dx &= \int_{\omega^\epsilon} c r dx, \quad r \in Q_h^{\omega^\epsilon}. \end{aligned} \quad (8)$$

For boundary conditions, we set

$$\phi_j \cdot n = 0, \quad x \in \partial\omega^\epsilon$$

and

$$\phi_j \cdot n = 0, \quad x \in \partial\mathcal{B}_e,$$

where n is the outward unit-normal vector on $\partial\omega^\epsilon$.

On the coarse edge E , we set the additional boundary condition

$$\phi_j \cdot n = \delta_j,$$

where $j = 1, J_{\omega^\epsilon}$ and number of local problems is $2 \cdot J_{\omega^\epsilon}$. Here J_{ω^ϵ} is the number of fine grid edges e_j on E , $E = \cup_{j=1}^{J_{\omega^\epsilon}} e_j$.

Next, we perform a space reduction on the snapshot space through the local spectral problem

$$\bar{A}_{\omega^\epsilon} \bar{\psi}_k^{\omega^\epsilon} = \lambda_k \bar{S}_{\omega^\epsilon} \bar{\psi}_k^{\omega^\epsilon}, \quad (9)$$

where

$$\begin{aligned} \bar{A}_{\omega^\epsilon} &= R_{\omega^\epsilon} A_{\omega^\epsilon} R_{\omega^\epsilon}^T, \quad \bar{S}_{\omega^\epsilon} = R_{\omega^\epsilon} S_{\omega^\epsilon} R_{\omega^\epsilon}^T, \\ R_{\omega^\epsilon} &= [\phi_1, \dots, \phi_{J_{\omega^\epsilon}}]. \end{aligned}$$

and

$$\begin{aligned} A_{\omega^\epsilon} &= [a_{mn}^{\omega^\epsilon}], \quad a_{mn}^{\omega^\epsilon} = a_{\omega^\epsilon}(\phi_m, \phi_n) = \int_E k^{-1} (\phi_m \cdot n)(\phi_n \cdot n) ds, \\ S_{\omega^\epsilon} &= [m_{mn}^{\omega^\epsilon}], \quad s_{mn}^{\omega^\epsilon} = s_{\omega^\epsilon}(\phi_m, \phi_n) = \int_{\omega^\epsilon} k^{-1} \phi_m \phi_n dx + \int_{\omega^\epsilon} \nabla \cdot \phi_m \nabla \cdot \phi_n dx. \end{aligned}$$

We arrange the eigenvalues in increasing order, and choose the first M_{ω^ϵ} eigenvalues and take the corresponding eigenvectors $\psi_k^{\omega^\epsilon} = R_{\omega^\epsilon} \bar{\psi}_k^{\omega^\epsilon}$ to be the basis functions, $k = 1, 2, \dots, M_{\omega^\epsilon}$.

Next, we define a multiscale space for the velocity filed using constructed multiscale basis functions

$$V_{ms} := \text{span}\{\psi_k^{\omega_i^\epsilon}, 1 \leq k \leq M_{\omega_i^\epsilon}, 1 \leq i \leq N_c\},$$

and define an projection matrix

$$R = \begin{bmatrix} R_u & 0 \\ 0 & R_p \end{bmatrix}, \quad R_u = [R_{u,1}, \dots, R_{u,N_E}]^T, \quad (10)$$

where $R_{u,i} = [\psi_1^{\omega_i^\epsilon}, \dots, \psi_{M_{\omega_i^\epsilon}}^{\omega_i^\epsilon}]^T$ and R_p is the projection matrix for pressure that contains constant on coarse cell for each row. Here N_E is the number of coarse grid edges and $M_{\omega_i^\epsilon}$ is the number of the local multiscale basis functions.

Using constructed multiscale space, we have following coarse-scale system in matrix form

$$\begin{pmatrix} A_c & B_c^T \\ B_c & 0 \end{pmatrix} \begin{pmatrix} u_c \\ p_c \end{pmatrix} = \begin{pmatrix} 0 \\ 0 \end{pmatrix}, \quad (11)$$

where

$$A_c = R_u A R_u^T, \quad B_c = R_u B R_p^T.$$

Using coarse-scale solution u_c , we can reconstruct fine-grid solution $u_{ms} = R_u^T u_c$ and use u_{ms} for the solution of the transport problem. [3, 10, 11, 4]

NUMERICAL RESULTS

We consider numerical simulation using the presented method in computational domain $\Omega_\epsilon = [0, L_x] \times [0, L_y]$ with $L_x = L_y = 1$. In Figure 3, we present coarse and fine grids for perforated domain. The fine mesh, that resolve perforations explicitly, contains 14648 vertices, 43087 facets and 28410 cells. We consider two coarse grids: (1) 10×10 grid with 36 vertices, 60 facets and 25 cells; (2) 5×5 grid with 121 vertices, 220 facets and 100 cells.

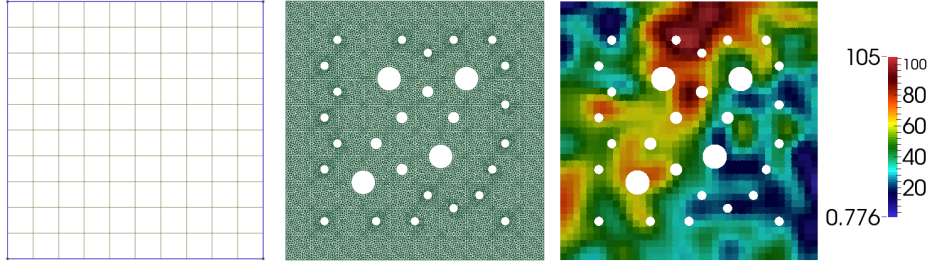


FIGURE 3. Coarse grid, fine grids and heterogeneous permeability. Left: coarse 10×10 grid with 121 vertices, 220 facets and 100 cells. Middle: fine grid with 14648 vertices, 43087 facets and 28410 cells. Right: heterogeneous permeability

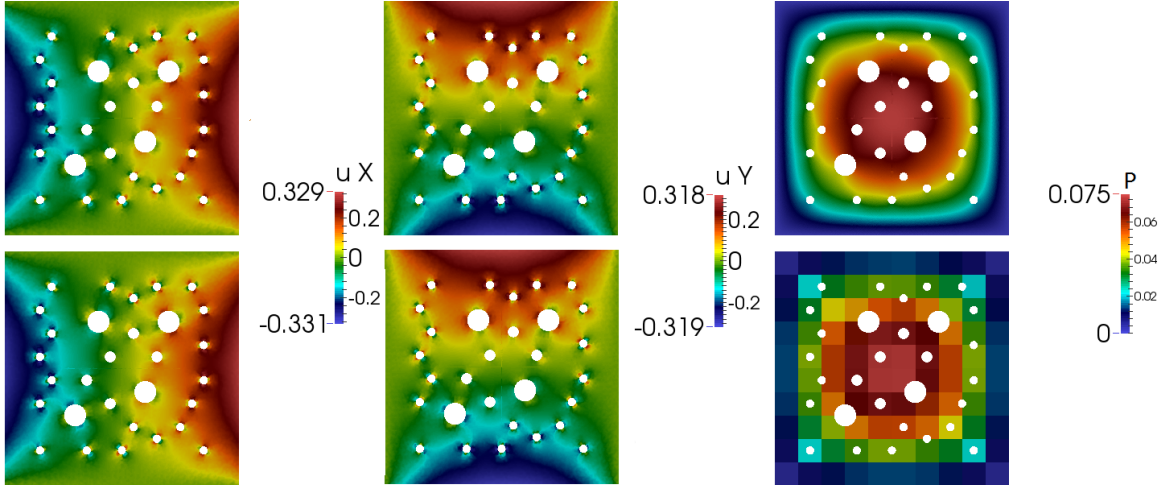


FIGURE 4. The distribution of X and Y components of the velocity and pressure in perforated domain (u_x - first column, u_y - second column and p - pressure). First row: fine grid solution, $DOF_f = 43058$. Second row: multiscale solution on 10×10 coarse grid using 4 multiscale basis functions for velocity, $DOF_c = 980$. *Test 1* with homogeneous permeability

We consider two test cases:

- *Test 1* with homogeneous permeability, $k = 1$.
- *Test 2* with heterogeneous permeability, $k = k(x)$ (Figure 3).

For source term, we set $f(x) = g$ for $x = 0.5, y = 0.5$ and $f(x) = 0$ else, where $g = 1$ for *Test 1* and $g = 0.1$ for *Test 2*. We set the initial conditions for $c(x, 0) = 1.0, \mu = 1$ and $D = 0.0001$. We perform simulations for $T_{max} = 1.5$ with $\tau = 0.01$ for *Test 1* and for $T_{max} = 9$ with $\tau = 0.1$ for *Test 2*.

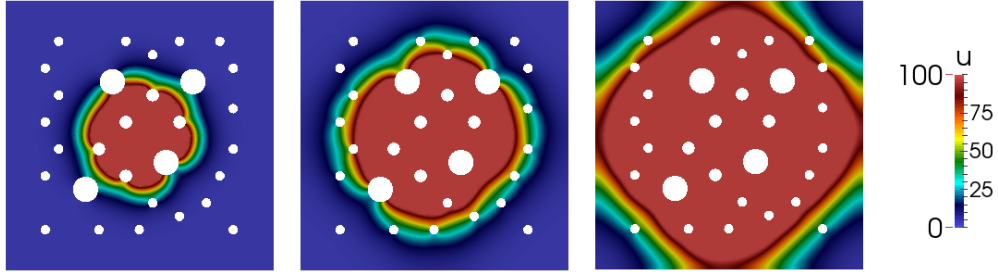


FIGURE 5. Fine grid solution of the transport equation in perforated domain for $t = 0.45, 0.9$ and 1.5 . *Test 1* with homogeneous permeability

TABLE 1. Relative errors for velocity, pressure and concentration with different number of multiscale basis functions for velocity, pressure and transport. *Test 1* with homogeneous permeability. Top: 5×5 coarse grid. Bottom: 10×10 coarse grid

M	DOF_c	$e_{L_2}^u$ (%)	$e_{H_1}^u$ (%)	$e_{L_2}^p$ (%)	$e_{L_2}^c$ (%)	$e_{H_1}^c$ (%)
Coarse grid 5×5						
1	85	4.166	0.133	6.968	1.629	1.534
2	145	0.180	0.005	6.790	0.009	0.007
3	205	0.094	0.003	6.790	0.004	0.002
4	265	0.037	0.001	6.790	0.0002	0.0001
Coarse grid 10×10						
1	320	1.077	0.034	1.821	0.642	0.800
2	540	0.063	0.002	1.829	0.312	0.056
3	760	0.009	0.0002	1.829	0.009	0.024
4	980	0.003	0.0001	1.829	0.003	0.007

TABLE 2. Relative errors for velocity, pressure and concentration with different number of multiscale basis functions for velocity, pressure and transport. *Test 2* with heterogeneous permeability. Top: 5×5 coarse grid. Bottom: 10×10 coarse grid

M	DOF_c	$e_{L_2}^u$ (%)	$e_{H_1}^u$ (%)	$e_{L_2}^p$ (%)	$e_{L_2}^c$ (%)	$e_{H_1}^c$ (%)
Coarse grid 5×5						
1	85	6.569	0.005	7.272	12.405	6.871
2	145	0.731	0.0005	6.857	3.723	2.036
3	205	0.354	0.0002	6.852	0.080	0.056
4	265	0.094	0.0001	6.790	0.003	0.001
Coarse grid 10×10						
1	320	2.921	0.002	2.174	5.177	3.768
2	540	0.326	0.0002	2.064	0.390	0.674
3	760	0.139	0.0001	2.063	0.008	0.041
4	980	0.046	0.00002	2.053	0.002	0.005

To compare the results, we use the relative L_2 error between fine-scale solutions v_f and multiscale solutions v_m s

for velocity, pressure and transport

$$e_{L_2}^2 = \frac{\int_{\Omega_e} |v_f - v_{ms}|^2 dx}{\int_{\Omega_e} |v_f|^2 dx}$$

and the relative H_1 error for velocity

$$e_{H_1}^2 = \frac{\int_{\Omega_e} (|v_f - v_{ms}|^2 + |\nabla \cdot (v_f - v_{ms})|^2) dx}{\int_{\Omega_e} (|v_f|^2 + |\nabla \cdot v_f|^2) dx}$$

and for transport

$$e_{H_1}^2 = \frac{\int_{\Omega_e} |\nabla(v_f - v_{ms})|^2 dx}{\int_{\Omega_e} |\nabla v_f|^2 dx}$$

The results of calculations in the perforated domain for *Test 1* with homogeneous permeability are shown in Figures 4 and 5. In Figure 4, we present X and Y components of velocity and pressure distributions for the numerical solution using GMsFEM and using fine grid approximation. Calculations were performed using 4 multiscale basis functions. In Figure 5, we present the transport distributions for $t = 0.45, 0.9$ and 1.5 using fine grid approximation. Relative L_2 and H_1 errors for velocity, concentration and L_2 pressure error are shown in Table 1 for 5×5 and 10×10 coarse grids. For example, if we use 1 multiscale basis functions for *Test 2* for 5×5 coarse grid, we get the following relative error velocity $e_{L_2}^2 = 4.166$ and for transport $e_{L_2}^2 = 1.629$. With an increase in the number of multiscale basis functions, the error decreases. And if we use 4 multiscale basis functions for 5×5 coarse grid, we get the relative error velocity $e_{L_2}^2 = 0.037$ and for transport $e_{L_2}^2 = 0.003$.

Next, we consider *Test 2* with heterogeneous permeability. In Table 2, we present relative errors for 5×5 and 10×10 coarse grids with different number of the multiscale basis functions. For example, if we use 1 multiscale basis functions for *est 2* for 5×5 coarse grid, we get the relative error velocity $e_{L_2}^2 = 6.569$ and for transport $e_{L_2}^2 = 12.405$. And if we use 4 multiscale basis functions, we get the relative error velocity $e_{L_2}^2 = 0.046$ and for transport $e_{L_2}^2 = 0.002$.

We considered numerical simulation with homogeneous and heterogeneous permeability. The numerical results show that one need around 4 basis functions to achieve a good accuracy. In Future works, we will consider three-dimensional problems in perforated domains.

ACKNOWLEDGEMENTS

The work is supported by the mega-grant of the Russian Federation Government No 14.Y26.31.0013 and RFBR N 17-01-00732.

REFERENCES

- [1] E.T. Chung, W.T. Leung, M. Vasilyeva, and Y. Wang (2018) Multiscale model reduction for transport and flow problems in perforated domains, *Journal of Computational and Applied Mathematics* **330**, 519–535.
- [2] E.T. Chung, W.T. Leung, and M. Vasilyeva (2016) Mixed GMsFEM for second order elliptic problem in perforated domains, *Journal of Computational and Applied Mathematics* **304**, 84–99.
- [3] E.T. Chung, Y. Efendiev, G. Li, and M. Vasilyeva (2016) Generalized multiscale finite element methods for problems in perforated heterogeneous domains, *Applicable Analysis* textbf95(10), 2254–2279.
- [4] E.T. Chung, M. Vasilyeva, and Y. Wang, A conservative local multiscale model reduction technique for Stokes flows in heterogeneous perforated domains, [arXiv:1608.07268](https://arxiv.org/abs/1608.07268), 2016.
- [5] K. Gao *et al* (2015) Generalized multiscale finite-element method (GMsFEM) for elastic wave propagation in heterogeneous, anisotropic media, *Journal of Computational Physics* **295**, 161–188.
- [6] E.T. Chung, Y. Efendiev, and W.T. Leung (2014) Generalized multiscale finite element methods for wave propagation in heterogeneous media, *Multiscale Modeling & Simulation* **12**(4), 1691–1721.

- [7] M. Vasilyeva and D.A. Stalnov, “Numerical averaging for the heat conduction problem in inhomogeneous and perforated media” (Herald of M.K. Ammosov Northeastern Federal University, 2017), No 2 (58). [in Russian]
- [8] A. Logg, K.A. Mardal, and G. Wells (Eds), *Automated Solution of Differential Equations by the Finite Element Method: The FEniCS Book* (Springer Science and Business Media, 2012), vol. 84.
- [9] Y. Efendiev and T. Hou, *Multiscale Finite Element Methods, Theory and Applications* (Springer, New York, 2009).
- [10] E.T. Chung *et al* (2017) Online adaptive local multiscale model reduction for heterogeneous problems in perforated domains, *Applicable Analysis* **96**(12), 2002–2031.
- [11] C. Le Bris, F. Legoll, and A. Lozinski (2014) An MsFEM type approach for perforated domains, *Multiscale Modeling & Simulation* **12**(3), 1046–1077.